Online Supplementary Material

BET Bromodomain Inhibition Attenuates Cardiac Phenotype in Myocyte-Specific Lamin A/C-Deficient Mice

Gaelle Auguste [1], Leila Rouhi[1], Scot J Matkovich,[2], Cristian Coarfa [3], Matthew J. Robertson [3], Grazyna Czernuszewicz [1], Priyatansh Gurha [1], Ali J. Marian [1 *]

[1] Center for Cardiovascular Genetics, Institute of Molecular Medicine and Department of Medicine,

University of Texas Health Sciences Center at Houston, Texas 77030

[2] Washington University, Saint Louis, MO

[3] Baylor College of Medicine, Houston, TX 77030

Address for Correspondence:
AJ Marian, M.D.
Center for Cardiovascular Genetics
6770 Bertner Street
Suite C900A
Houston, TX 77030
713 500 2350
Ali.J.Marian@uth.tmc.edu

Material and Methods

The studies conformed to the Guide for the Care and Use of Laboratory Animals published by the US National Institutes of Health and were approved by the Animal Care and Use Committee and the Biological Safety Committee of the University of Texas Health Science Center-Houston.

***Myh6-Cre:Lmna*$^{F/F}$, *Myh6-Cre:Lmna*$^{W/F}$ and wild type (WT) littermates:** *Myh6-Cre:Lmna*$^{F/F}$, *Myh6-Cre:Lmna*$^{W/F}$ and age- and sex-matched WT mice were used in these experiments, the latter as controls. *Myh6-Cre* and *Lmna*$^{F/F}$ mice were included as control in the phenotype characterization. The *Myh6-Cre* deleter mice were crossed to *Lmna*$^{F/F}$ mice to generate *Myh6-Cre:Lmna*$^{F/F}$ and *Myh6-Cre:Lmna*$^{W/F}$ mice. (1, 2) Expression of the Cre recombinase is expected to delete the LoxP-flanked exon 2 of *Lmna* gene in the heart only in cells expressing *Myh6, i.e.*, cardiac myocytes. Mice were housed in a 12-hours light/night cycle facility with *ad libidum* food and water. DNA extracted from tail-clip was used for genotyping. Oligonucleotide primers used in PCR reactions are listed in Table S7.

Survival: Survival of the *Myh6-Cre:Lmna*$^{F/F}$, *Myh6-Cre:Lmna*$^{W/F}$, *Myh6-Cre*, *Lmna*$^{F/F}$ and WT mice was analyzed by constructing Kaplan-Meier survival plots.

Gross morphology: *Myh6-Cre:Lmna*$^{F/F}$, *Myh6-Cre:Lmna*$^{W/F,}$, *Myh6-Cre*, *Lmna*$^{F/F}$ and WT mice were weighted every other day and body weight (BW) recorded.

Echocardiography and Electrocardiography (EKG): Cardiac size and function were assessed in age- and sex-matched mice by 2D, M mode, and Doppler echocardiography, as published using a Vevo 1100 ultrasound imaging system equipped with a 22-55 MHz MicroScan transducer (MS550D) (FUJIFILM VisualSonics Inc., Toronto, ON, Canada). (3-5)

Echocardiography was performed in 2-weeks old WT and *Myh6-Cre:Lmna*$^{F/F}$ and in 3-week old WT, *Myh6-Cre, Lmna*$^{F/F}$, *Myh6-Cre:Lmna*$^{W/F}$**,** and *Myh6-Cre:Lmna*$^{F/F}$ mice. Echocardiography was also repeated in 8 to 10 months old WT, *Myh6-Cre,* and *Myh6-Cre:Lmna*$^{W/F}$ mice. Mice were anesthetized and maintained under anesthesia throughout the procedure using 0.5-1% isoflurane and positioned on a heating pad in supine position. Chest hair was removed using a hair removal cream. ECG and respiratory rate were recorded during the measurement**.** Wall thicknesses and left ventricular dimensions were measured from

M-mode images from the parasternal two-dimensional short-axis view at the tip of the mitral leaflet, using the leading-edge method. Left ventricular fractional shortening and mass were calculated from the measured indices. Echocardiographic data were measured in 5-6 cardiac cycles and mean values were used.

Surface ECG was obtained by using subcutaneous needle-electrodes inserted into the upper precordial area. During the recording, mice were kept lightly anesthetized using 0.5-1% isoflurane and under constant monitoring on a 37 °C heated pad. Leads were connected to a PowerLab 4/30 System using an Animal Bio Amp module (ADInstruments, Colorado Springs, CO, USA), and data were recorded and Analyzed using LabChart7 Software. Echocardiograms and ECG were analyzed without knowledge of the genotype.

Isolation of cardiac myocytes: Cardiac myocytes were isolated as published. (5) Briefly, mice were anesthetized with intraperitoneal injection of pentobarbital (62 mg/Kg I.P.). Anesthetized mice were injected intraperitoneally with 200 units of Heparin and the heart was excised and placed in a Ca^{2+} free perfusion buffer [120 mM NaCl, 15 mM KCl, 0.6 mM KH_2PO_4, 0.6 mM Na_2HPO_4, 1.2 mM $MgSO_{47}H_2O$, 30 mM Taurine, 4.6 mM $NaHCO_3$, 10 mM HEPES, 10 mM 2,3-Butanedione monoxime (BDM), and 5.5 mM Glucose; pH 7.0]. The heart was cannulated through ascending aorta, with the cannula was positioned above the aortic valves, and was connected to a retrograde perfusion system. The heart was perfused with the perfusion buffer at a constant rate of 4 mL/min until blood was fully rinsed. Then, Collagenase II (Worthington, Lakewood, NJ) at 250 units/mL was added to the buffer, and the heart was perfused for 2 to 3 minutes before supplementation with 12.5 µM $CaCl_2$. The perfusion was continued until complete softening of the myocardium. The heart was then minced into small pieces in the digestion buffer, and cells were dissociated by gentle pipetting. Upon complete dissociation of the tissue, calf serum (10% in final volume) was added to stop the enzymatic digestion, and the cell suspension was passed through a 100 µm nylon mesh. Myocytes were left to sediment by gravity in the presence of 2 mM ATP and pelleted by centrifugation at 20 g for 3 minutes. Sequential concentrations of calcium (100 µM, 400 µM, and 900 µM), were re-introduced to the cells in presence of 2 mM ATP. The final isolate was washed once in PBS, pelleted at low speed and immediately frozen for future protein and RNA experiments.

Histology: Mice were euthanized by carbon dioxide inhalation followed by cervical dislocation. Hearts were rapidly excised, rinsed twice with ice-cold Phosphate Buffered Saline (PBS), and dry-blotted before cross sectioning and being placed in a neutral formalin solution overnight.

Myocardial thin sections (5-6 μm) were stained with Masson trichrome and Sirius Red (SR), as described. (4-6) Myocardial fibrosis was quantified by determining collagen volume fraction (CVF) in at least 10 high magnification fields (x40) per section and in a minimum of 3 sections per heart. The specific number of animals used in each experimental group was indicated in the figure legend. Images were analyzed using the ImageJ software.

Immunofluorescence (IF): IF was performed as previously described. (3-6) A detailed list of antibodies used in these experiments is provided in Table S7. Briefly, after harvest, the hearts were placed in optimal cutting temperature compound (OCT, Fisher 23-730-571) and snap- frozen using cold 2-Methylbutane. Freshly sectioned cardiac cross-sections were fixed for 5 min at room temperature in 4% formaldehyde. After extensive washes, sections were blocked in 5% donkey serum with PBS and 0.3% Triton X-100 for 1 hour at room temperature before overnight incubation at 4°C with the primary antibodies in 1% bovine serum albumin (BSA) in PBS and 0.3% Triton-X-100 solution. Sections were then incubated with appropriated secondary antibody conjugated with fluorescent dyes. Nuclei were counterstained with 0.1 mg/mL of 4′, 6 Diamidino-2-phenylindole dihydrochloride (DAPI, Sigma-Aldrich St Louis, MO; cat# D8417). Slides were mounted using a fluorescent mounting medium (Dako cat# S3023). Sections were then examined with an inverted fluorescent microscope (Zeiss, Axioplan Fluorescence Microscope). Image acquisition was performed with AxioVision software. Iterative deconvolution was performed on Z-stack acquired images at high magnification (X100). Quantification were performed in at least 10 high magnification fields (x40) per section and a minimum of 3 sections per heart. For LMNA quantification, an average of 6,420 DAPI positive nuclei and 1,740 PCM1-labeled/DAPI-positive nuclei were examined. The specific number of animals used in each experimental group was indicated in the figure legend. Images were analyzed using the ImageJ software and the AxioVision software.

Detection of apoptosis: Apoptosis was detected by nick-end labelling of DNA with the TUNEL assay using In Situ Cell Death Detection Kit (Roche catalogue # 11684795910), per manufacturer instructions, as described. (3-6) In brief, paraffin embedded thin myocardial sections were dewaxed and treated with Proteinase K (10 mg/ml in 10 mM Tris/HCl, pH 7.5) for 20 min at 37°C before incubation with the TUNEL reaction mixture for 1 hour at 37°C. Nuclei were counterstained with DAPI. Visualization and image acquisition were performed using an Axioplan fluorescence microscope (Zeiss). TUNEL positive cells were quantified in a minimum of 10 high magnification fields (x40) per section, 3-4 thin sections per each heart,. Percentage of TUNEL-positive nuclei was determined in each group in an average of 16,500 DAPI-positive nuclei in 2-week old mice, 6,400 DAPI-positive nuclei in 3-week old mice, and 12,000 DAPI-positive nuclei in the JQ1-study. The specific number of mice used in each experimental group was indicated in the figure legend.

Reverse transcription-Quantitative real-time PCR (RT-qPCR): Total RNA was extracted using the Qiagen miRNeasy Mini Kit (catalogue # 217004) from myocardial tissue or from isolated cardiac myocytes. DNase treatment was performed to eliminate contaminating genomic DNA. High Capacity cDNA Reverse Transcription Kit (Life tech, catalogue # 4368814) was used to generate cDNAs. Transcript levels were determined by RT-qPCR using specific TaqMan gene expression assays or SYBR Green specific primers, and normalized to glyceraldehyde-3-phosphate dehydrogenase (*Gapdh*) mRNA levels. All reactions were performed in duplicates or triplicates and in four to seven mice per group. The specific number of animals used in each experimental group is indicated in the figure legend. The ΔCT method was used to calculate the normalized gene expression value (normalized to *Gapdh*). Statistical analysis for the gene expression data was performed using the non-normalized ΔCT values. Data in the experimental groups were presented as fold change relative to the control samples. Taqman probes and SYBR Green primers are detailed in Table S7.

Immunoblotting: Protein levels in mouse heart samples and isolated cardiac myocytes were detected and quantified by immunoblotting. Briefly, tissues were lysed in a RIPA buffer (PIERCE, Rockford, IL, catalogue #89900) containing protease and phosphatase inhibitors (cØmplete and phosSTOP;

Roche Molecular Biochemicals, catalogue # 11-873-580-001 and # 04-906-837-001, respectively). The samples were homogenized using a hand-held homogenizer and lysed on a rotator at 4 °C for 20 minutes. Cell debris were pelleted by centrifugation at 12,000 rpm for 15 min at 4 °C. The pellet was resuspended in the RIPA buffer supplemented with 1% final SDS, homogenized, and were sonicated for 30 seconds. The protein concentration was measured by Bio-Rad DC Protein Assay Kit (Bio-Rad Laboratories, # 5000111), or Bradford (Abcam #119216). Protein extracts were heated in a Laemmli buffer at 95 °C for 5 min and 30 to50 µg of each protein extract was loaded onto SDS/PAGE gels, separated by electrophoresis, and transferred to nitrocellulose membranes. The membranes were probed with primary antibodies against the proteins of interest and the corresponding HRP conjugated secondary antibodies (the list of the antibodies is provided in Table S7). Signals were detected by chemiluminescence using the LI-COR Odyssey Fc imaging system (LI-COR Biotechnology). Membranes were stripped of the antibodies upon incubation in Restore PLUS Western Blot Stripping Buffer (Thermo Scientific, Hudson, New Hampshire, catalogue #46430) at room temperature, and then were re-probed with an antibody against the loading control protein GAPDH. Intensity of the specific bands was quantified using in-build Licor system Image Studio Lite Ver 5.2. Each lane read out was normalized to its corresponding band of the loading control. Data in the experimental groups were presented as the fold change relative to the control samples.

RNA-Sequencing (RNA-Seq): Total RNA was isolated from cardiac myocytes of 2 and 3week old WT and *Myh6-Cre*:*Lmna*$^{F/F}$ mice. RNA-seq was performed on ribosome-depleted RNA on an Illumina platform, as published.(3-6) In brief, ribosome-depleted RNA was extracted from isolated cardiac myocytes and analyzed for integrity on an Agilent Bioanalyser RNA chip. Samples with an RNA Integrity Number (RIN) read out of more than 8 were used to prepare sequencing library using the Illumina TruSeq stranded total RNA library preparation kit. The samples were sequenced on the Illumina HiSeq 4000 instrument using the paired-end sequencing reagents to generate 75 and 100 base pair runs.

Raw RNA sequencing reads were mapped and aligned to the Mouse reference genome build 10 (UCSC mm10/GRCm38) using Tophat2. (7) Gene counts were obtained using the HT-Seq (8) and differential expression was determined using the edgeR and voom and using DESeq2 with RUV (Removed unwanted variation) normalization (9, 10) and annotated using the GENCODE gene model (https://www.gencodegenes.org/mouse/). Normalized counts were presented as count per million (CPM).

Quality control and data visualization were assessed by principal components analysis (PCA) and heatmaps from the CPM values with unsupervised hierarchical clustering were performed by Clustvis (https://biit.cs.ut.ee/clustvis/). Graph Pad Prism was used to generate the volcano plots. Enriched upstream regulators were inferred using the Ingenuity Pathway Analysis® (IPA, Qiagen) with Z score cut-off set at ≤2 or ≥ -2.

Pathway analysis for the DEG was performed using the Gene Set Enrichment Analysis (GSEA, version 2.2.3, http://software.broadinstitute.org/gsea/) on the ranked gene list. (11)

BRD4 activation status found in the 2 weeks old RNA-Seq was further validated against BRD4 target genes reported in 4 independent public datasets. BRD4 target genes were defined as genes whose expressions were induced in the cardiac pathological conditions but suppressed upon inhibition of BRD4. The public databases included mouse hearts (mmuHeart-1 GSE48110, mmuHeart-2 TAC GSE96561, and mmuHeart-3 MI GSE96561) and neonatal rat cardiomyocytes (NRVM-1 GSE48111). (12, 13) BRD4 core target genes were defined upon pooling the GSEA core enrichment of DEGs in *Myh6-Cre:Lmna*$^{F/F}$ myocytes against those in the 4 BRD4 target data sets. (12, 13) Differentially expressed genes encoding for secreted proteins were obtained as described. (14)

ChIP-Seq: Isolated myocytes were resuspended in PBS immediately after the last step of calcium reintroduction. Protein DNA complexes were crossed linked with 1% formaldehyde at room temperature for 5 minutes. Then, 125mM of glycine at was added to each sample to quench the reaction. The cells were then washed 3 times in PBS and lysed using a Dounce on ice in a cell lysis buffer (5mM Na-Butyrate, 10mM HEPES pH8.0, 85mM KCl, 0.6% NP-40, protease and phosphatase inhibitors). The lysates were centrifugated for 5 minutes at 2,000 rpm at 4ºC, resuspended in the cell lysis buffer, and incubated on ice for 10 minutes. The percentage of free nuclei was assessed visually, the suspension was centrifugated, and resuspended in nuclear lysis buffer (50mM Tris-HCl pH 8.0, 10mM EDTA, 1% Triton X-100, 0.8% SDS, protease and phosphatase inhibitors). The lysates were homogenized and incubated for 10 minutes on ice with regular flicking, and sonicated on a Bioruptor Pico for 20 cycles of 30 sec ON/30 sec OFF at +4ºC. The sheared chromatin was collected after centrifugation for 10 minutes at +4ºC at 13,000 rpm, and diluted 10-fold with ChIP dilution buffer (16.7mM Tris-HCl, 1.2mM EDTA, 140mN NaCl, 1.1% Triton X-100 protease and phosphatase inhibitors). A 10% input was collected before adding 6µg of an anti-BRD4 antibody to the sheared chromatin. After overnight immunoprecipitation, a mixture of 1% BSA pre-blocked sepharose G beads, , was added onto each sample for 1 hours. Immunoprecipitates were then washed sequentially with a Low Salt buffer (0.1% SDS, 1%TritonX-100, 2mM EDTA, 20mM Tris-HCl pH 8.0, 150mM NaCl), High Salt buffer (0.1% SDS, 1%TritonX-100, 2mM EDTA, 20mM Tris-HCl pH 8.0, 500mM NaCl), LiCl buffer (1% NP-40, 1% Na-Deoxycholate, 1mM EDTA, 10mM Tris-HCl pH8.0, 250mM LiCl), and twice in TE buffer (10mM Tris-HCl pH 8.0, 1mM EDTA). The chromatin was eluted in 1% SDS, 10mM EDTA, 50mM Tris-HCl pH 8.0 at +65ºC for 15 minutes with agitation and was then agitated at +65 ºC overnight with 200mM final of NaCl. The chromatin was treated with RNAse A for 2 hours at +37ºC, proteinase K for 1 hour at +55ºC, and the DNA was then extracted using Phenol/chloroform extraction and ethanol precipitation. The DNA concentration was assessed using the High Sensitivity Qubit, and the size on an Agilent Bioanalyser DNA chip. Libraries were prepared using the Kapa Hyper Kit and single read of 50 bp length were sequenced on a HiSeq 3000.

Sequencing of BRD4 ChIP-Seq libraries yielded 36-65 million single-end reads. Reads were aligned to the mm10 release of the mouse genome by Bowtie v 2.3.4.3. Only uniquely mapping reads were selected for further analysis. ChIP-seq peaks were called using MACS2 from Galaxy (Version 2.1.1). (15) Region of BRD4-ChIP enrichment over background were identified using the default parameters. Enriched regions were intersected using Bedtool function Multiple Intersect (Galaxy Version 2.27.1) and regions present in at least two samples per genotype were considered as BRD4-bound regions (q<0.05). Data was deposited in GEO (Accession # GSE142129).

Overlapping BRD4 bound regions were represented as Venn diagrams. The relative location of BRD4 peaks, genomic distribution of BRD4 bound regions, and the nearest annotated genes to BRD4 peaks were assigned using the PAVIS tool (https://manticore.niehs.nih.gov/pavis2/#). (16) BRD4 bound regions that were present in the *Myh6-Cre:Lmna*$^{F/F}$ samples and absent in the WT samples were assigned as Gain of Peak (GoP) and those that were unique to WT were assigned as Loss of Peak (LoP) for further analysis.

The frequency and distribution of the transcript levels in the BRD4 bound region were compared to those that are not bound and presented as violin plots using R (https://cran.r-project.org/). Likewise, density plots for the transcript levels and fold change genome wide and in the GoP and LoP regions were plotted using R and density plots and sort map function in EaSeq (http://easeq.net. (17)

ChIP-qPCR: Validation of ChIP-Seq was performed using an independent ChIP using anti-BRD4 antibody on CM obtained from WT and *Mhy6-cre:Lmna*$^{F/F}$ as described above and processed as for the ChIP-Sequencing. Genomic regions showing enrichment for BRD4 were visualized using Integrative Genomics Viewer (IGV), and sequences flanking the enriched regions were used to design primers. (18) Quantitative PCR was performed to evaluate enrichment of BRD4 in the WT and *Mhy6-cre:Lmna*$^{F/F}$ sample using Sybr Green primers that are listed in the Online Table 8.

Statistical analyses: Normality of data distribution was assessed by Shapiro-Wilk's test. Data that followed a Gaussian distribution pattern were presented as mean ± SD and compared using unpaired t-test, ordinary One-Way ANOVA, or two-way ANOVA, followed with Tukey or Bonferroni multiple comparison test, as appropriate. Otherwise, data were presented as the median values and compared by Kolmogorov-Smirnov, Kruskal-Wallis, or Mann-Whitney test followed with Dunn's test correction for multiple comparison. Survival rates were analyzed by constructing Kaplan-Meier survival plots and comparing the survival rate by Log-rank (Mantel-Cox) test.

References

1. Agah R, Frenkel PA, French BA, Michael LH, Overbeek PA, and Schneider MD. Gene recombination in postmitotic cells. Targeted expression of Cre recombinase provokes cardiac-restricted, site-specific rearrangement in adult ventricular muscle in vivo. *J Clin Invest.* 1997;100(1):169-79.
2. Kim Y, and Zheng Y. Generation and characterization of a conditional deletion allele for Lmna in mice. *Biochem Biophys Res Commun.* 2013;440(1):8-13.
3. Chen SN, Lombardi R, Karmouch J, Tsai JY, Czernuszewicz G, Taylor MRG, et al. DNA Damage Response/TP53 Pathway Is Activated and Contributes to the Pathogenesis of Dilated Cardiomyopathy Associated With LMNA (Lamin A/C) Mutations. *Circ Res.* 2019;124(6):856-73.
4. Cheedipudi SM, Hu J, Fan S, Yuan P, Karmouch J, Czernuszewicz G, et al. Exercise Restores Dysregulated Gene Expression in a Mouse Model of Arrhythmogenic Cardiomyopathy. *Cardiovasc Res.* 2019.
5. Auguste G, Gurha P, Lombardi R, Coarfa C, Willerson JT, and Marian AJ. Suppression of Activated FOXO Transcription Factors in the Heart Prolongs Survival in a Mouse Model of Laminopathies. *Circ Res.* 2018.
6. Karmouch J, Zhou QQ, Miyake CY, Lombardi R, Kretzschmar K, Bannier-Helaouet M, et al. Distinct Cellular Basis for Early Cardiac Arrhythmias, the Cardinal Manifestation of Arrhythmogenic Cardiomyopathy, and the Skin Phenotype of Cardiocutaneous Syndromes. *Circ Res.* 2017;121(12):1346-59.
7. Kim D, Pertea G, Trapnell C, Pimentel H, Kelley R, and Salzberg SL. TopHat2: accurate alignment of transcriptomes in the presence of insertions, deletions and gene fusions. *Genome Biol.* 2013;14(4):R36.
8. Anders S, Pyl PT, and Huber W. HTSeq--a Python framework to work with high-throughput sequencing data. *Bioinformatics.* 2015;31(2):166-9.
9. Law CW, Chen Y, Shi W, and Smyth GK. voom: Precision weights unlock linear model analysis tools for RNA-seq read counts. *Genome Biol.* 2014;15(2):R29.
10. Frankish A, Diekhans M, Ferreira AM, Johnson R, Jungreis I, Loveland J, et al. GENCODE reference annotation for the human and mouse genomes. *Nucleic Acids Res.* 2019;47(D1):D766-D73.
11. Subramanian A, Tamayo P, Mootha VK, Mukherjee S, Ebert BL, Gillette MA, et al. Gene set enrichment analysis: a knowledge-based approach for interpreting genome-wide expression profiles. *Proc Natl Acad Sci U S A.* 2005;102(43):15545-50.
12. Duan Q, McMahon S, Anand P, Shah H, Thomas S, Salunga HT, et al. BET bromodomain inhibition suppresses innate inflammatory and profibrotic transcriptional networks in heart failure. *Sci Transl Med.* 2017;9(390).
13. Anand P, Brown JD, Lin CY, Qi J, Zhang R, Artero PC, et al. BET bromodomains mediate transcriptional pause release in heart failure. *Cell.* 2013;154(3):569-82.
14. Cheedipudi SM, Matkovich SJ, Coarfa C, Hu X, Robertson MJ, Sweet M, et al. Genomic Reorganization of Lamin-Associated Domains in Cardiac Myocytes Is Associated With Differential Gene Expression and DNA Methylation in Human Dilated Cardiomyopathy. *Circ Res.* 2019;124(8):1198-213.
15. Zhang Y, Liu T, Meyer CA, Eeckhoute J, Johnson DS, Bernstein BE, et al. Model-based analysis of ChIP-Seq (MACS). *Genome Biol.* 2008;9(9):R137.

16. Huang W, Loganantharaj R, Schroeder B, Fargo D, and Li L. PAVIS: a tool for Peak Annotation and Visualization. *Bioinformatics.* 2013;29(23):3097-9.
17. Lerdrup M, Johansen JV, Agrawal-Singh S, and Hansen K. An interactive environment for agile analysis and visualization of ChIP-sequencing data. *Nat Struct Mol Biol.* 2016;23(4):349-57.
18. Robinson JT, Thorvaldsdottir H, Winckler W, Guttman M, Lander ES, Getz G, et al. Integrative genomics viewer. *Nat Biotechnol.* 2011;29(1):24-6.

Supplementary Figures and Figure legends

Online Figure 1: LMNA levels in the *Lmna*$^{F/F}$ cardiac myocytes and in the *Myh6-Cre*:*Lmna*$^{F/F}$ mice non-myocyte cardiac fraction:

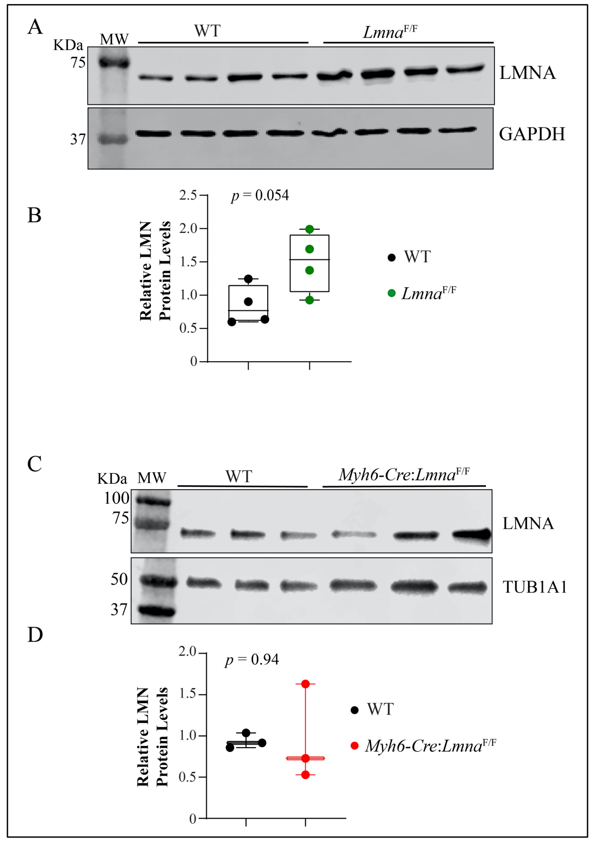

Immunoblot (IB) of LMNA in cardiac myocytes protein lysates from *Lmna*$^{F/F}$ mice, and the corresponding

TUBA1A, as loading control (A). Corresponding quantitation of LMNA expression levels in the WT (N=4) and *Lmna*$^{F/F}$ (N=4) is shown in Panel B (unpaired t test, p=0.54).

C. Immunoblot (IB) of LMNA in non-myocyte cardiac fraction protein lysates from WT and *Myh6-Cre*:*Lmna*$^{F/F}$ mice, and the corresponding GAPDH, as a loading control. Corresponding quantitation of LMNA expression levels in the WT (N=3) and *Myh6-Cre*:*Lmna*$^{F/F}$ (N=3, unpaired t test, test *p*=0.94) (D).

Online Figure 2: Body weight plots over time in the experimental groups:

Graph showing time course changes in body weight in the wild type (WT), *Myh6-Cre*:*Lmna*$^{W/F}$, *Lmna*$^{F/F}$, *Myh6-Cre,* and *Myh6-Cre*:*Lmna*$^{F/F}$ mice (*P* values were calculated using two-way ANOVA followed with Bonferroni's multiple comparisons *post-hoc* test, and were as follows: $p_{\text{Interaction}}<0.0001$, $p_{\text{Age}}<0.0001$, $p_{\text{Genotype}}<0.0001$. Significance for each comparison is denoted as * $p < 0.0001$ *Lmna*$^{F/F}$, *Myh6-Cre* or *Myh6-Cre*:*Lmna*$^{W/F}$ *vs* WT mice; # $p < 0.0001$ *Myh6-Cre*:*Lmna*$^{F/F}$ *vs* WT mice; † $p < 0.0001$ *Myh6-Cre*:*Lmna*$^{W/F}$ *vs Lmna*$^{F/F}$ or *Myh6-Cre*; ‡ $p<0.0001$ *Myh6-Cre*:*Lmna*$^{F/F}$ *vs Lmna*$^{F/F}$; ° $p < 0.0001$ *Myh6-Cre vs Myh6-Cre*:*Lmna*$^{W/F}$; \$ $p < 0.0001$ *Myh6-Cre vs Myh6-Cre*:*Lmna*$^{F/F}$; and § $p < 0.0001$ *Myh6-Cre*:*Lmna*$^{F/F}$ *vs Myh6-Cre*:*Lmna*$^{W/F}$.

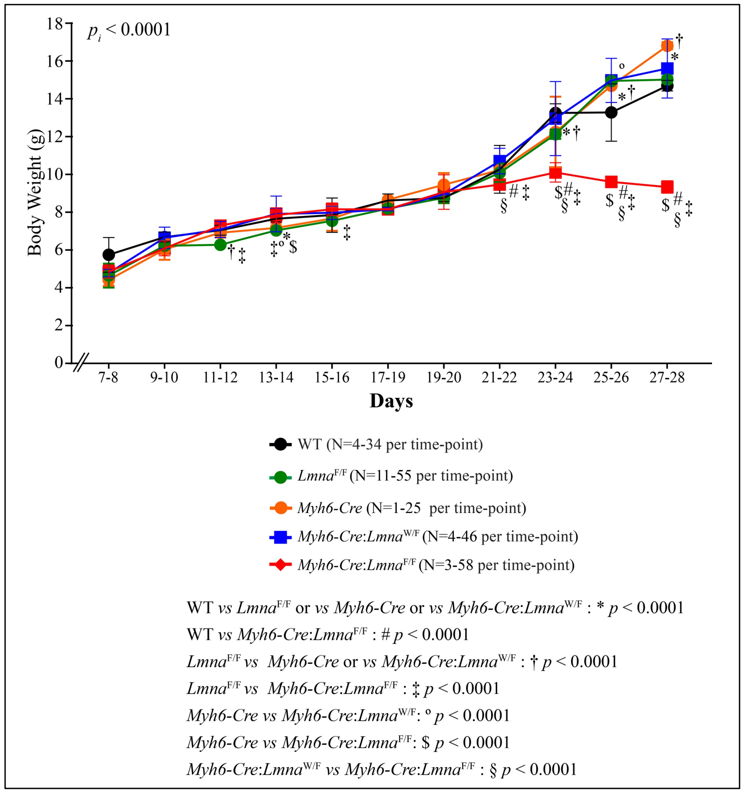

Online Figure 3: Survival of male and female *Myh6-Cre*:*Lmna*$^{F/F}$ mice: Kaplan-Meyer plot showing the survival of WT and *Myh6-Cre*:*Lmna*$^{F/F}$ male and female mice. Log-rank (Mantel-Cox) test was used to compare WT male (N=26), WT female (N=22), *Myh6-Cre*:*Lmna*$^{F/F}$ male (N=23) and *Myh6-Cre*:*Lmna*$^{F/F}$ female (N=22) (X^2=52.58, p <0.0001). *Myh6-Cre*:*Lmna*$^{F/F}$ male and female mice were compared alone (X^2=0.28, p<0.59).

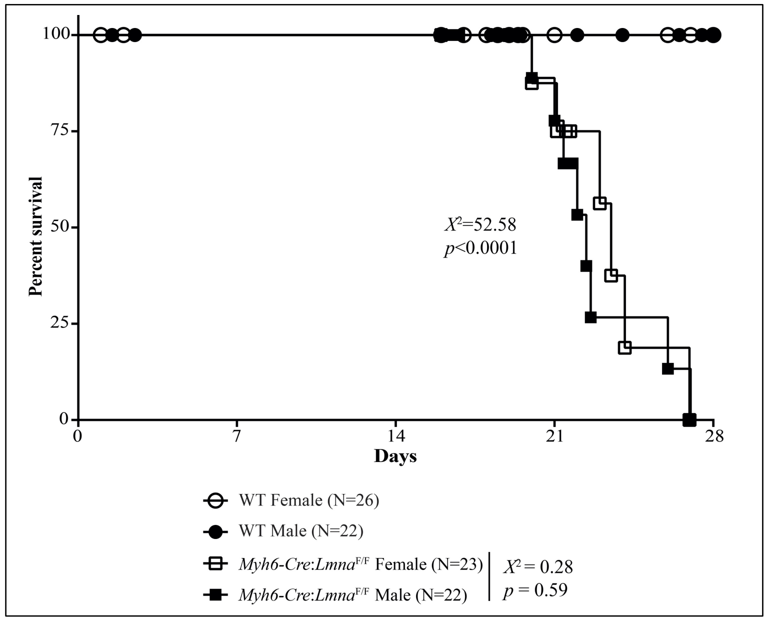

Online Figure 4: Echocardiographic indices of cardiac function in male and female wild type (WT) and Myh6-Cre:LmnaF/F mice: Selected echocardiographic parameters in 3 week-old WT male (N=6), WT Female (M=7), *Myh6-Cre*:*Lmna*$^{F/F}$ male (N=8) and *Myh6-Cre*:*Lmna*$^{F/F}$ female (N=9) mice showing body weight (A), Heart weight indexed to the body weight (B), left ventricular end-diastolic diameter indexed to body weight (LVEDDi), left ventricular end-systolic diameter (LVESD), left ventricular fractional shortening (LVFS). P value were obtained using ANOVA and Bonferroni pairwise comparison or Kruskal-Wallis test.

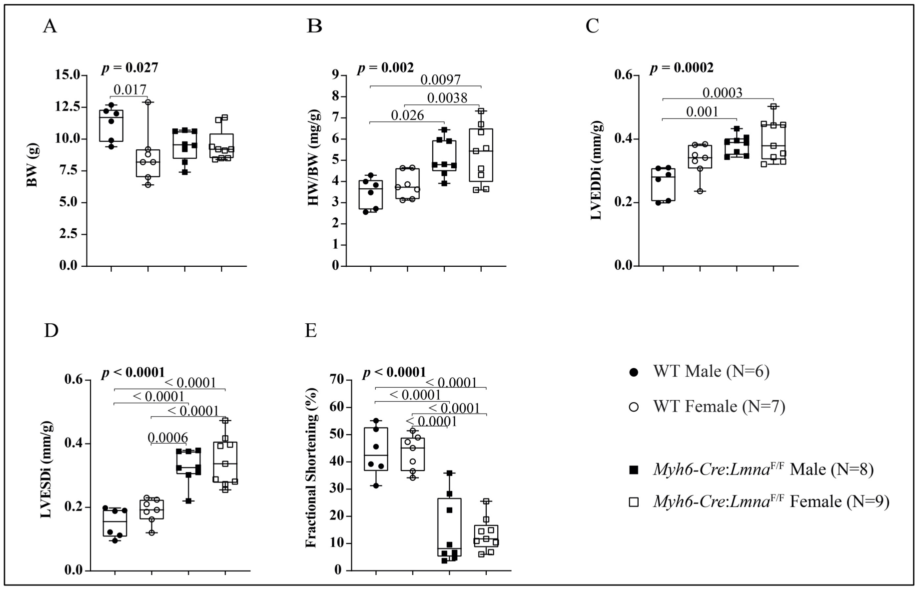

Online Figure 5: Myocardial histology and apoptosis in 8 to 10-month old WT and *Myh6-Cre*:*Lmna*$^{W/F}$ mice.

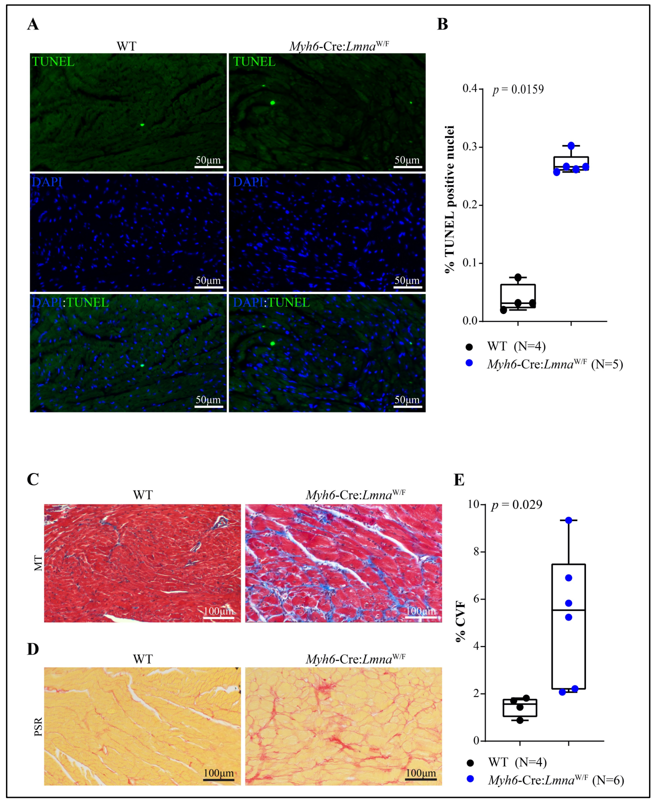

TUNEL staining (green) of representative myocardial sections in 8 to 10 months-old WT and *Myh6-Cre*:*Lmna*$^{W/F}$ mice. Nuclei (blue) were counterstained with DAPI (A). Corresponding quantitative data showing percentage of TUNEL-labelled and DAPI positive nuclei in WT (N=4) and *Myh6-Cre*:*Lmna*$^{W/F}$ (N=5) mouse hearts. *P* value (p=0.016) was calculated using Mann-Whitney statistical test (B). **C** and **D.** Masson's Trichrome (C) and Picrosirius red (D) stained representative myocardial sections in 8 to 10 months-old WT and *Myh6-Cre*:*Lmna*$^{W/F}$ mice. Corresponding quantitative data of percentage of collagen volume fraction (CVF) in the myocardial sections in WT (N=4) and *Myh6-Cre*:*Lmna*$^{W/F}$ (N=6) mouse hearts is shown. *P* value (p=0.029) was calculated by unpaired T-test (E).

Online Figure 6: Myocardial histology in 3 weeks old the *Lmna*$^{F/F}$ mice: Picrosirius red (stained representative myocardial sections in 3 week-old WT and *Myh6-Cre*:*Lmna*$^{W/F}$ mice (A). Corresponding quantitative data of percentage of collagen volume fraction (CVF) in the myocardial sections in WT (N=5) and *Lmna*$^{F/F}$ (N=5) mouse hearts is shown. *P* value (*p*=0.063) was calculated by unpaired t test (E).

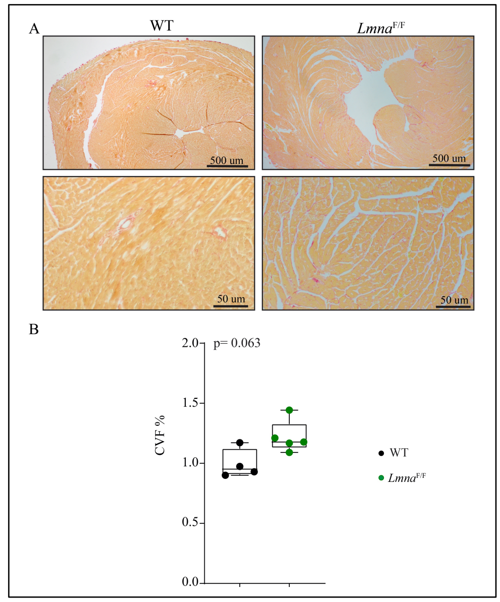

Online Figure 7: Myocardial histology and apoptosis in 2-week old WT and *Myh6-Cre*:*Lmna*$^{W/F}$ mice.

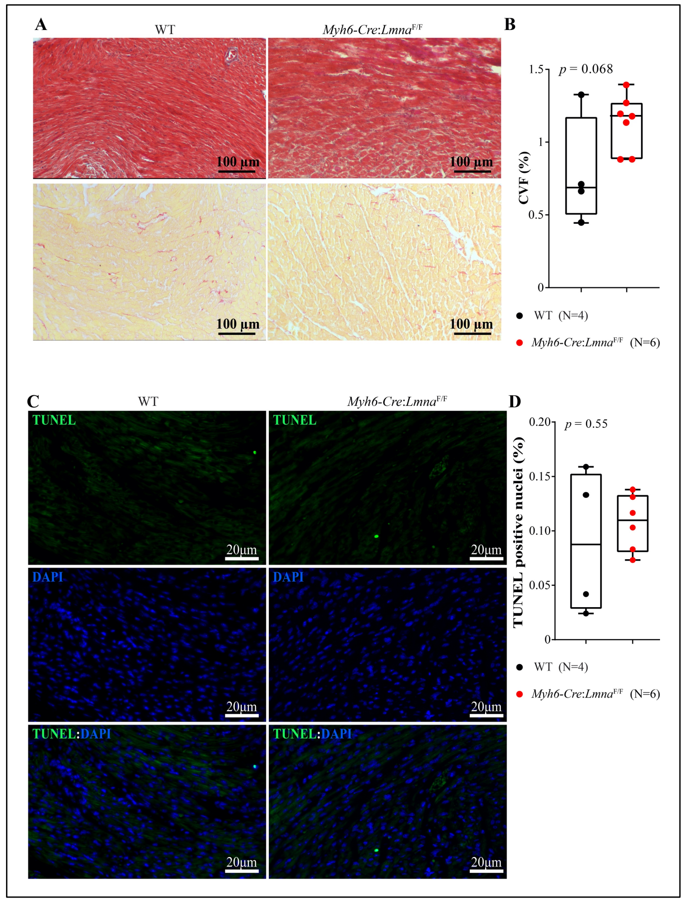

Masson's Trichrome (upper panels) and Picrosirius red (lower panels) stained representative myocardial sections in 2-week old WT and *Myh6-Cre*:*Lmna*$^{F/F}$ mice (A). Corresponding quantitative data of collagen volume fraction (CVF) as percent of myocardial sections in WT (N=4) and *Myh6-Cre*:*Lmna*$^{F/F}$ (N=6) mouse hearts are shown (B). TUNEL stained (in green) representative myocardial sections in 2-week old WT and *Myh6-Cre*:*Lmna*$^{F/F}$ mice. Nuclei (blue) were counterstained with DAPI (C). Corresponding quantitative data showing percentage of TUNEL-labelled nuclei (DAPI positive) in WT (N=4) and *Myh6-Cre*:*Lmna*$^{F/F}$ (N=6) mouse hearts is shown. *P* values were calculated by unpaired t test (D).

Online Figure 8: Principal Component Analysis plots of RNA Sequencing Data in 2-week old cardiac myocytes:

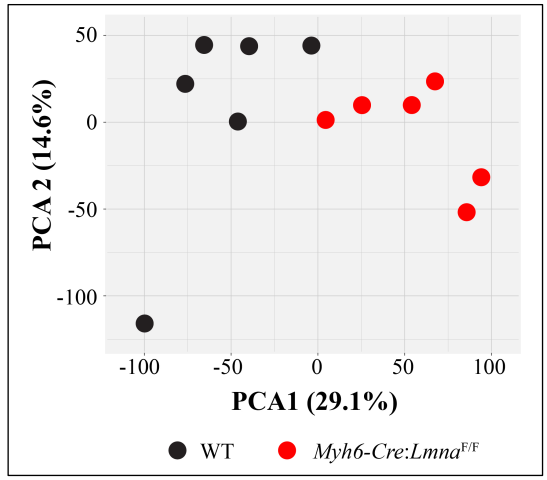

Principal component analysis of the RNA-Seq performed on 2-week old cardiac myocytes in WT (black, N=6) and *Myh6-Cre*:*Lmna*$^{F/F}$ (red, N=6) mice.

Online Figure 9: Secretome in 2 and 3 week-old cardiac myocytes in *Myh6-Cre:Lmna*$^{F/F}$ mice.

Heat map and unsupervised hierarchical clustering of the 168 differentially expressed secreted factors in 2 week-old cardiac myocytes in WT (N=6) and *Myh6-Cre:Lmna*$^{F/F}$ (N=6) mice (A). RT-qPCR data showing selected transcript level of secreted genes that were induced (B) or decreased (C) in 3-week old cardiac myocytes. Transcripts levels were confirmed on mRNA extracted from an independent set of *Myh6-Cre:Lmna*$^{F/F}$ mouse cardiac myocytes samples from the one used in the RNA-sequencing. Experimental groups are: WT (black, N=6) and *Myh6-Cre:Lmna*$^{F/F}$ (red, N=7) mice. T-test or Mann-Whitney were used to determine the statistical significance, where * p <0.05, ** $p < 0.01$, *** $p < 0.001$, **** $p < 0.0001$ (B-C). Ingenuity Pathway Analysis (IPA) for inferred activated and inhibited upstream regulators of the differentially expressed secreted factors in 2 week-old cardiac *Myh6-Cre:Lmna*$^{F/F}$ mouse cardiac myocytes. Z-score is represented for each upstream regulator (D) only ones that were significant are shown (Z score <2 or >-2 and a p<0.05). Gene set enrichment analysis (GSEA) plot of the TGFβ1 pathway in the 2 week-old *Myh6-Cre:Lmna*$^{F/F}$ mouse cardiac myocytes(Normalized score enrichment (NES)= 3 and $p < 0.001$ (E). IB of TGFβ on protein lysates from 3 week-old WT and *Myh6-Cre:Lmna*$^{F/F}$ cardiac myocytes showing TGF β latent form (around 50kDA) and TGB β active form (around 25kDA), with GAPDH as corresponding loading control (F). Corresponding

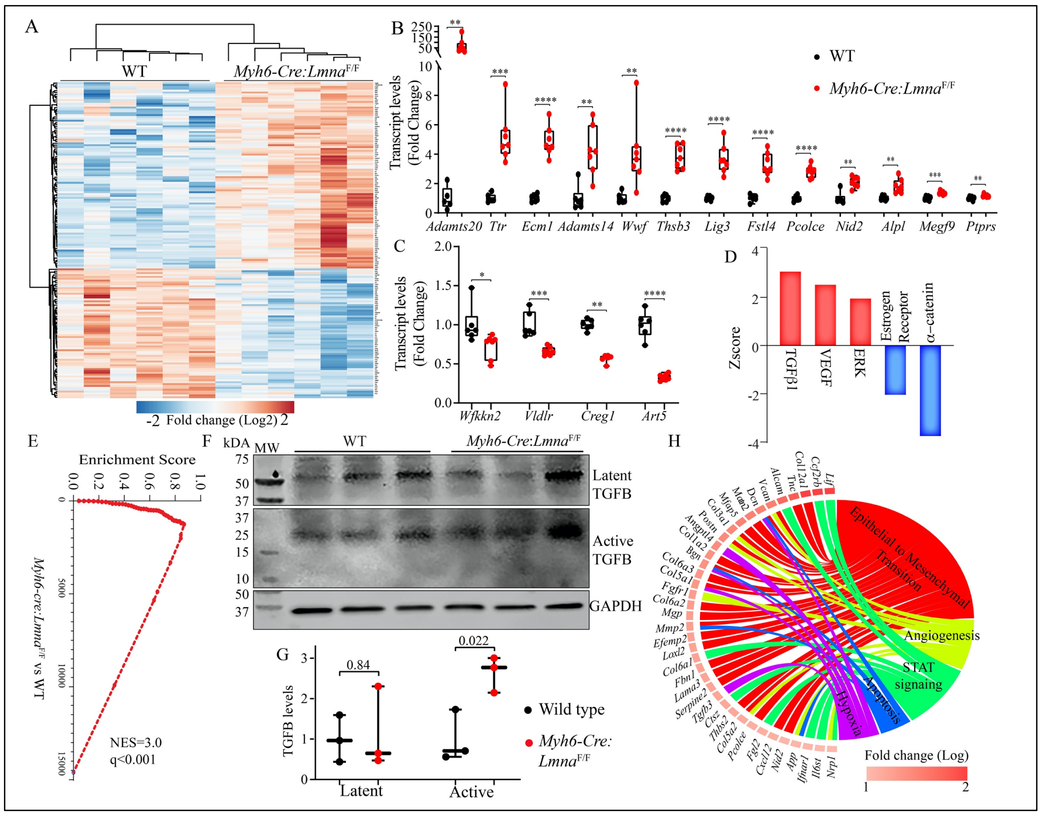

quantification of TGFB1 levels after normalization with GAPDH in 3 week-old WT (N=3) and *Myh6-Cre*:*Lmna*$^{F/F}$ (N=3) cardiac myocytes. *P* values were calculated by unpaired T-test (G). Circos Plot showing the top five significantly enriched Hallmark pathways inferred from the 168 secreted genes in 2 week-old in *Myh6-Cre*:*Lmna*$^{F/F}$ mouse cardiac myocytes using GSEA, with the log2 fold change depicting the relative expression of the genes involved in these pathways. (H).

Online Figure 10: Expression levels of BRD2, 3, and 4 proteins in 2 week-old cardiac myocytes.

IB of BRD2, BRD3 and BRD4 in protein lysates from 2 week-old WT and *Myh6-Cre*:*Lmna*$^{F/F}$ cardiac myocytes, with GAPDH as corresponding loading control (A). Corresponding quantification of BRD2, BRD3 and BRD4 levels after normalization with GAPDH in 3 weeks old WT (N=3) and *Myh6-Cre*:*Lmna*$^{F/F}$ (N=3) cardiac myocytes. *P* values were calculated by unpaired t test (B).

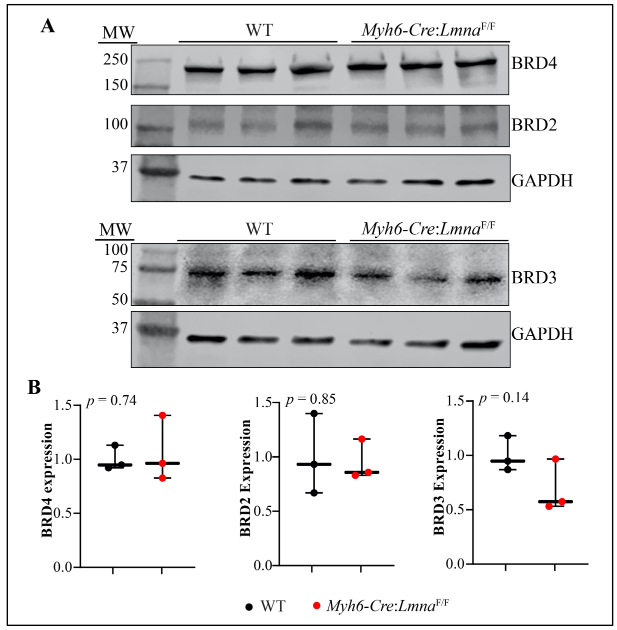

Online Figure 11: BRD4 Chromatin Immunoprecipitation-Sequencing (ChIP-Seq) data:

Four-way Venn diagram showing overlap of the BRD4 peaks present in each BRD4-ChIP sample in the WT and *Myh6-Cre*:*Lmna*$^{F/F}$ mouse cardiac myocytes. The corresponding number of BRD4 peaks is indicated within each respective area (A). Venn Diagram showing overlaps among peaks presents in the BRD4-ChIP-seq in the WT (N=4) and *Myh6-Cre*:*Lmna*$^{F/F}$ (N=4) mouse groups. Corresponding number of the peaks is indicated within each respective area (B). Venn Diagram showing the BRD4 peaks overlap between WT and *Myh6-Cre*:*Lmna*$^{F/F}$ for the peaks that were shared by at least 2 BRD4-ChIP-seq samples within the same genotype. The corresponding number of BRD4 peaks is indicated within each respective area (C). Pie chart depicting genomic partition of the BRD4 peaks for the annotated genes in the WT and *Myh6-Cre*:*Lmna*$^{F/F}$ mice. The corresponding number of peaks and their percentages relative to the total number of genes are shown in the pie charts (D).

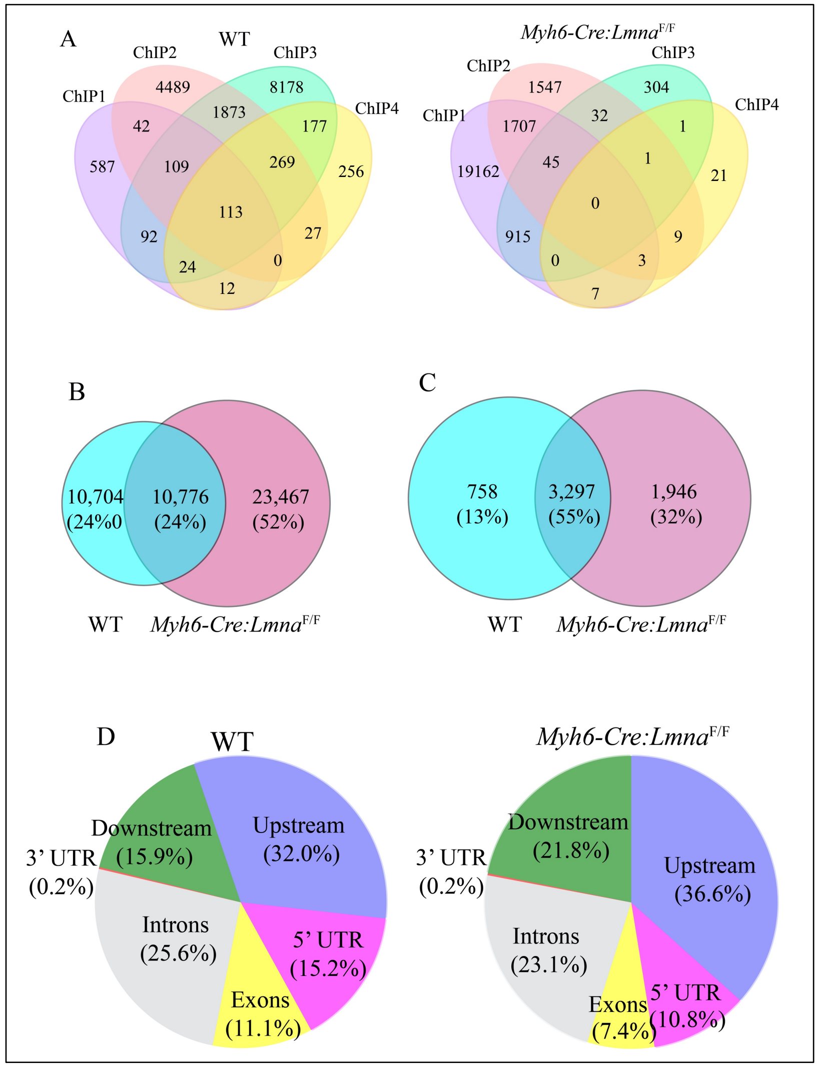

Online Figure 12: BRD4 Chromatin Immunoprecipitation-Sequencing (ChIP-Seq) data

Sort map showing transcript levels of genes (log10 of count per million- CPM) in the BRD4 Gain-of-Peak (GoP) and Loss-of-Peak (LoP) regions in the WT and *Myh6-Cre*:*Lmna*$^{F/F}$ mouse cardiac myocytes (A). Density plots showing the number of genes versus their transcript levels (fold change) in the GoL and LoL regions within 50 kb of the gene transcription starting site (TSS) in the *Myh6-Cre*:*Lmna*$^{F/F}$ mouse cardiac myocytes (B). Density plots showing the number of DEGs versus their transcript levels (fold-change) in the GoP and LoP regions in the *Myh6-Cre*:*Lmna*$^{F/F}$ mouse cardiac myocytes, within 50 kb of the gene TSS (left) and in the upstream region from the TSS (right) (C). Venn Diagram showing the overlap of the DEGs located at the BRD4 enriched region between WT and *Myh6-Cre*:*Lmna*$^{F/F}$ genome-wide, and per genomic partition (D). Bar graphs showing genomic partition of the DEGs annotated in GoP and LoP regions in the *Myh6-Cre*:*Lmna*$^{F/F}$ mice. The up-regulated DEGs are shown in red and the down-regulated in blue (E). p values are calculated by the Chi Square test.

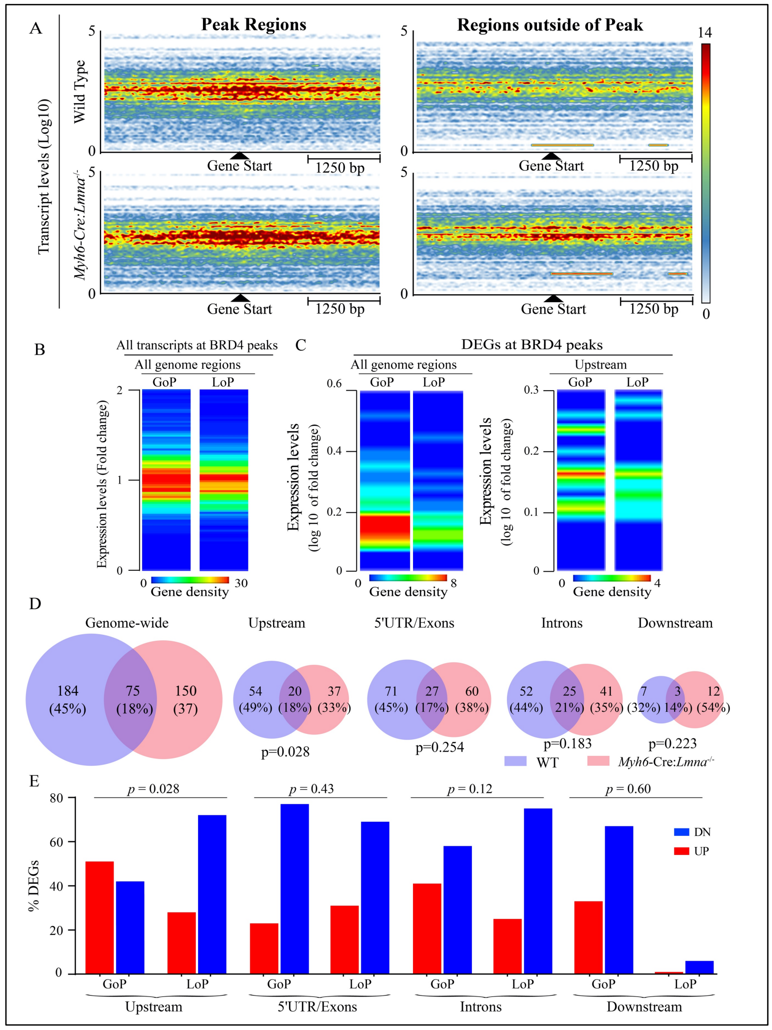

Online Figure 13: Phenotypic effects of conventional dose and age administration of JQ1 in WT mice.

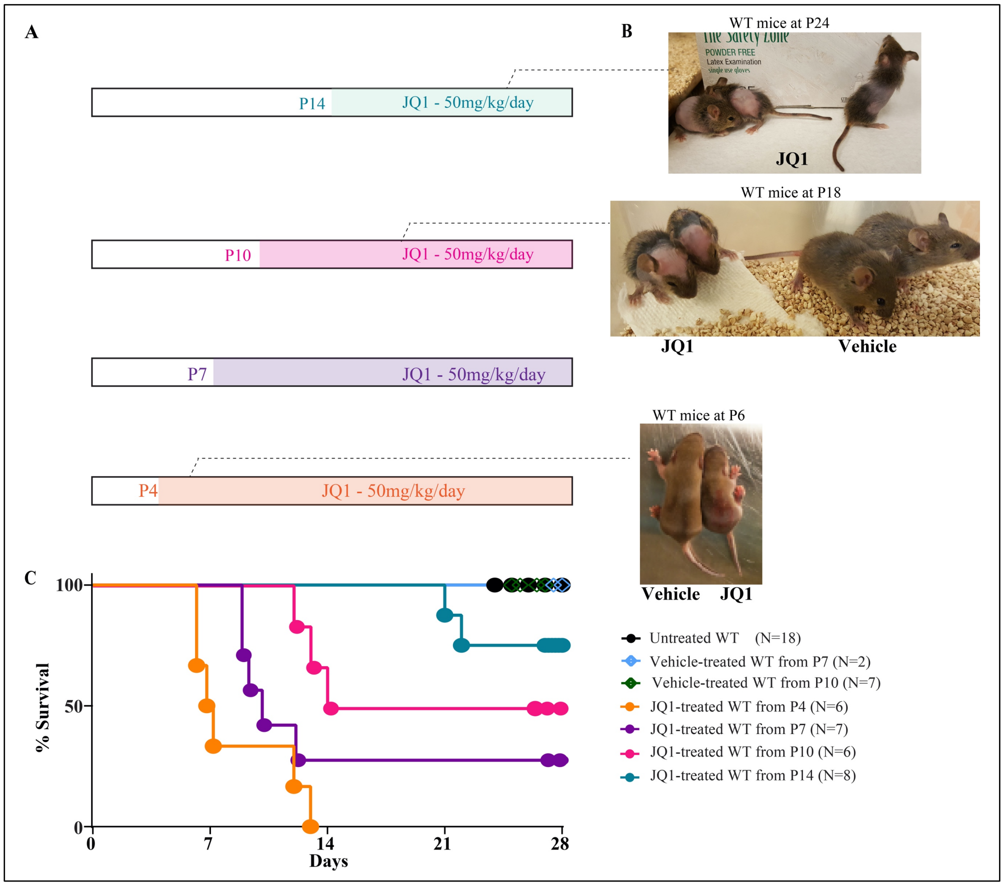

Vehicle (10% DMSO, 10% 2-Hydroxypropyl)-β-cyclodextrin) or JQ1 (50mg/Kg) was administered daily subcutaneously from post-natal day 4 (P4) in WT mice for a dose-titration study (orange curve, N=6), P7 (purple curve, N=7), P10 (pink curve, N=6) and P14 (teal curve, N=8) (A). Examples of toxic effects on JQ1 on hair loss and failure to thrive are shown (B). Corresponding Kaplan-Meier survival curve for each protocol is shown. Untreated WT (black curve, N=18), or vehicle-treated WT from P7 (light blue curve, N=2) or from P10 (olive green curve, N=7) survival plots are also depicted (C).

Online Figure 14: Effects of reduced dose of JQ1 on survival and body weight.

Effects of 20mg/Kg of JQ1 administered daily at P14 on survival. Survival of WT mice treated with the reduced dose of JQ1 was unchanged (A). Daily body weight recording in untreated WT mice, WT mice treated with the vehicle (10% DMSO, 10% 2-Hydroxypropyl)-β-cyclodextrin), and WT mice treated with JQ1 at 20mg/Kg/d starting at P14. The mice had normal gain-in-weight within the first 28 days of life (B).

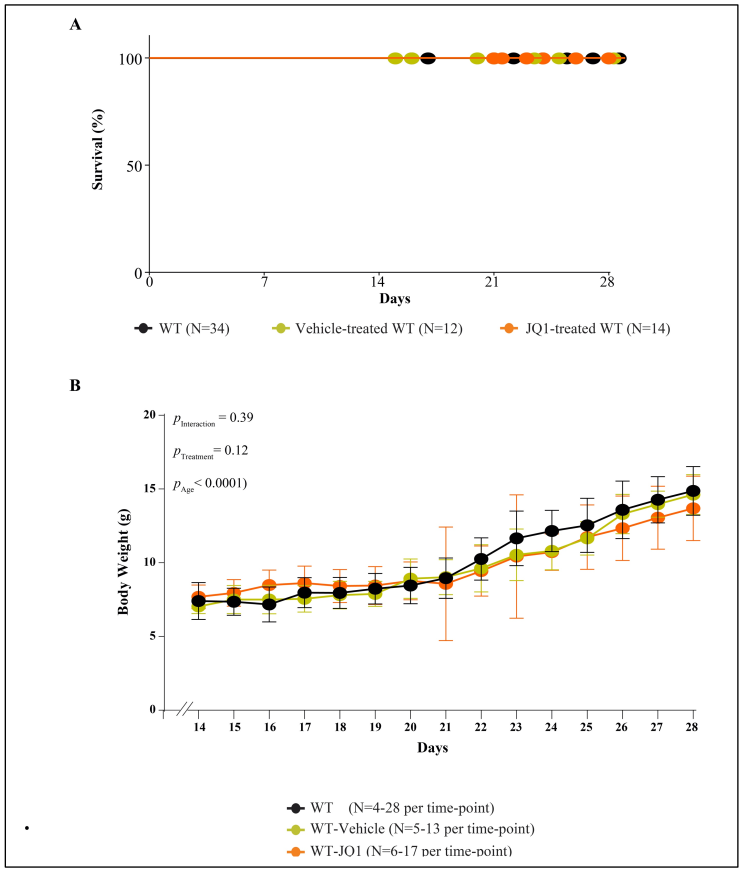

Online Figure 15: Reverse transcriptase-quantitative PCR (RT-qPCR) of additional BRD4 target genes.

RT-qPCR data showing transcript level of additional BRD4 target genes, which were reduced but not totally normalized upon JQ1-treatment in cardiac myocytes. Experimental groups are: untreated WT (black, N=6), untreated *Myh6-Cre*:*Lmna*$^{F/F}$ (red, N=6), and JQ1-treated *Myh6-Cre*:*Lmna*$^{F/F}$ (green, N=7) mice (A). Transcript levels of BRD4 target genes showing no effect of treatment with JQ1, as compared between untreated WT (black, N=6), untreated *Myh6-Cre*:*Lmna*$^{F/F}$ (red, N=6), and JQ1-treated *Myh6-Cre*:*Lmna*$^{F/F}$ (green, N=7) groups (B). Data were compared by one-way ANOVA followed with Bonferroni's multiple comparisons *post-hoc* test for normally distributed data and Kruskal-Wallis followed with Dunn's multiple comparisons *post-hoc* test for data deviating from normality. Respective level of significance for pairwise comparison are reported for each graph as follow * $p < 0.05$, ** $p < 0.01$, **** $p < 0.0001$.

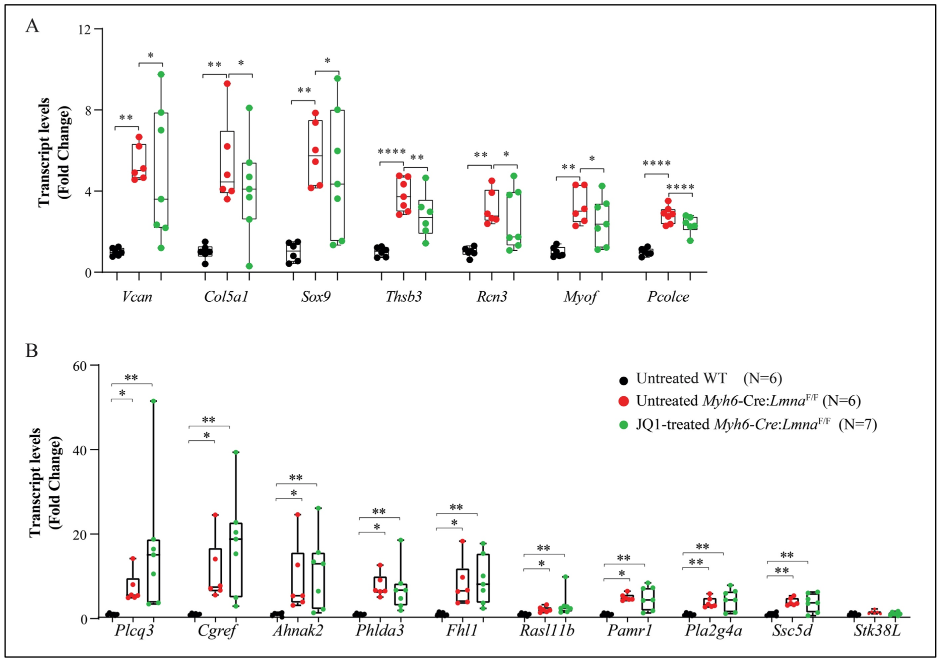

Figure Online 16: Effect of JQ1 on secretome in 3 week-old mice: Heat map and unsupervised hierarchical clustering of the 195 secreted factors differentially expressed in *Myh6-Cre*:*Lmna*$^{F/F}$ compared

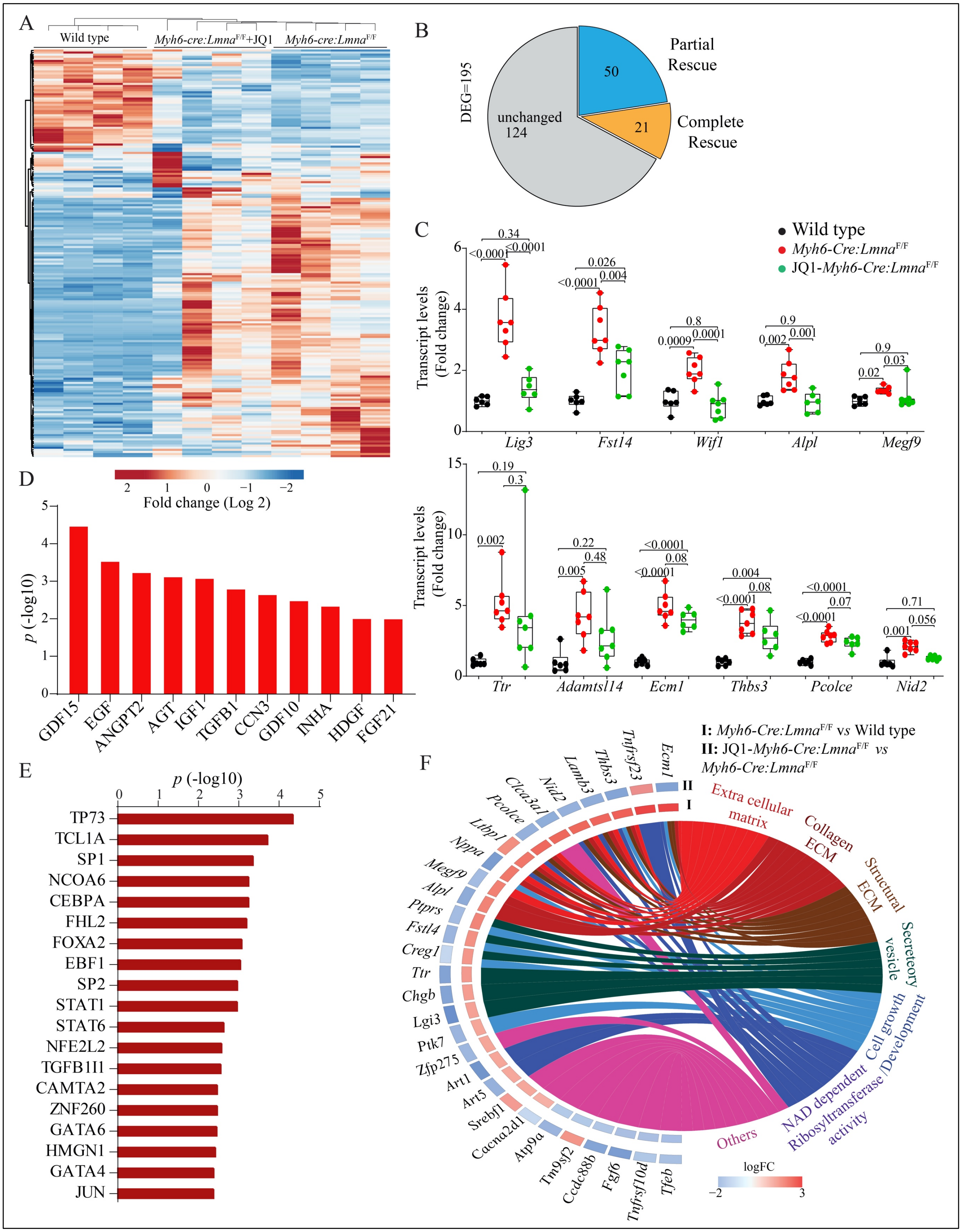

to WT (q<0.05) in 3 week-old WT (N=4) and *Myh6-Cre*:*Lmna*$^{F/F}$ (N=4), and JQ1-treated *Myh6-Cre*:*Lmna*$^{F/F}$ (N=4) mouse cardiac myocytes (A). Pie chart depicting the expression levels of the 195 secreted factors upon JQ1-treatment in *Myh6-Cre*:*Lmna*$^{F/F}$. Genes were considered as completely rescued if their expression was differential between JQ1-treated *Myh6-Cre*:*Lmna*$^{F/F}$ and *Myh6-Cre*:*Lmna*$^{F/F}$ (q<0.05), but not from the WT mice (q>0.05). They were considered partially rescued if their expression was differential between JQ1-treated *Myh6-Cre*:*Lmna*$^{F/F}$ and *Myh6-Cre*:*Lmna*$^{F/F}$ (q<0.05), and still different from the WT mice (q<0.05) or if there expression was not significant to WT and *Myh6-Cre*:*Lmna*$^{F/F}$. Gene were considered as unchanged if their expression was not different between JQ1-treated *Myh6-Cre*:*Lmna*$^{F/F}$ and *Myh6-Cre*:*Lmna*$^{F/F}$ (q<0.05) (B). RT-qPCR data showing transcript level of secreted genes selected from the rescued group, showing complete rescue (upper panel), or tending to rescue (lower panel) upon JQ1-treatment in *Myh6-Cre*:*Lmna*$^{F/F}$ cardiac myocytes. Experimental groups are: untreated WT (black, N=6), untreated *Myh6-Cre*:*Lmna*$^{F/F}$ (red, N=6), and JQ1-treated *Myh6-Cre*:*Lmna*$^{F/F}$ (green, N=7) mice. P values were obtained using one way ANOVA or Kruskal-Wallis, as appropriate (C). IPA analysis for upstream regulator showing top dysregulated growth factors (D) and Transcription regulators (E) inferred from the 195 differentially secreted factors (D-E). P values indicate the strength of overlap between the gene in rescued group to that in the corresponding IPA dataset. Circos plot of the differentially secreted factors showing the top GO term associated, with a comparison of their relative expression as follows **I:** *Myh6-Cre*:*Lmna*$^{F/F}$ *vs* WT, **II:** JQ1-treated *Myh6-Cre*:*Lmna*$^{F/F}$ *vs Myh6-Cre*:*Lmna*$^{F/F}$. Log2 fold change is color coded as indicated.

Online Figure 17: Effects of treatment with JQ1 on body weight of *Myh6-Cre*:*Lmna*$^{F/F}$ mice.

Body weight daily recording in untreated (black; N=4 to 28 per time-point), vehicle-treated (yellow; N=5-13) and JQ1-treated WT (orange; N=6-17), as well as untreated (red, N=2-30), vehicle-treated (blue; N=2-14) and JQ1-treated *Myh6-Cre*:*Lmna*$^{F/F}$ (green; N=7-13) mice. *P* values were obtained from two-way ANOVA ($p_{\text{Interaction}}$<0.0001, p_{Age}<0.0001, p_{Genotype}<0.0001) followed with Bonferroni's multiple comparisons *post-hoc* test.

* $p < 0.05$: Untreated WT vs untreated, Vehicle-treated or JQ1-treated *Myh6-Cre*:*Lmna*$^{F/F}$

\# $p < 0.05$: Vehicle-treated WT vs untreated, Vehicle-treated or JQ1-treated *Myh6-Cre*:*Lmna*$^{F/F}$

† $p < 0.05$: JQ1-treated WT vs untreated, Vehicle-treated or JQ1-treated *Myh6-Cre*:*Lmna*$^{F/F}$

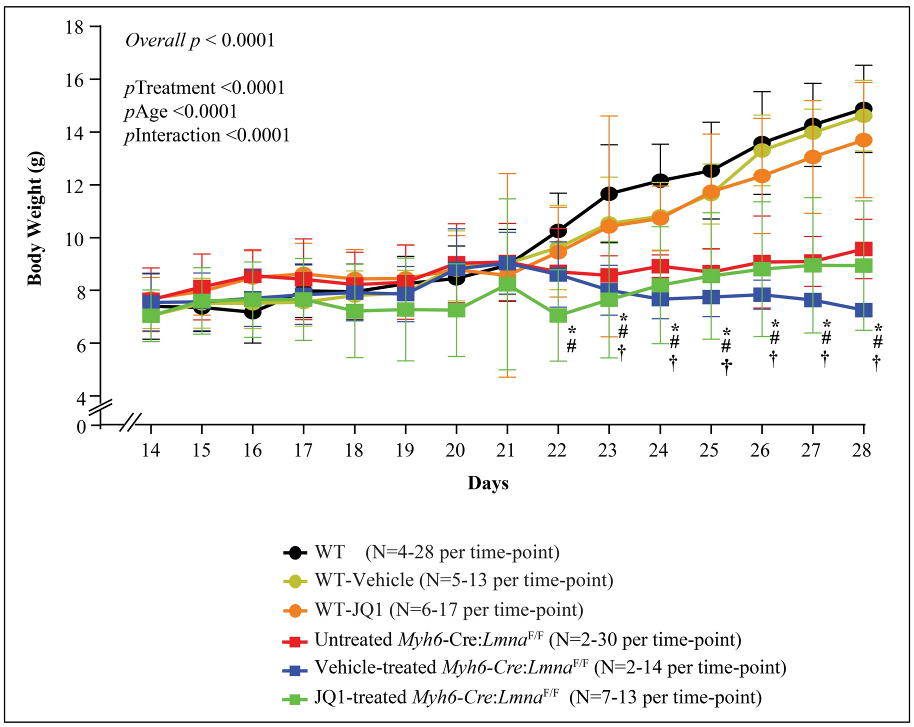

Supplementary Tables

Online Table 1

Echocardiographic parameters in WT, *Myh6-Cre, Lmna*$^{F/F}$, *Myh6-Cre:Lmna*$^{W/F}$ and *Myh6-Cre:Lmna*$^{F/F}$ mice at 3 weeks of age.

	WT	***Myh6*-Cre**	***Lmna*$^{F/F}$**	***Myh6*-Cre:*Lmna*$^{W/F}$**	***Myh6*-Cre:*Lmna*$^{F/F}$**	*p*
N	13	11	9	12	17	N/A
M/F	6/7	5/6	6/3	5/7	8/9	0.82$^{\chi}$
Age (days)	21.6 ± 0.5	21.9 ± 1.1	22 ± 0.7	21.2 ± 0.7	21.2 ± 1.3	0.15[b]
BW (g)	9.9 ± 2.2	9.9 ± 1.1	12.0 ± 2.1	10.6 ± 1.0	9.5 ± 1.2 †	0.013[b]
HR (bpm)	457 ± 49	468 ± 35	465 ± 32	473 ± 47	475 ± 75	0.77[b]
ST (mm)	0.58 ± 0.07	0.50 ± 0.08	0.48 ± 0.06	0.55 ± 0.13	0.54 ± 0.08	0.08[b]
PWT (mm)	0.58 ± 0.06	0.50 ± 0.05	0.52 ± 0.15	0.55 ± 0.12	0.53 ± 0.08	0.09[b]
LVEDD (mm)	2.87 ± 0.39	3.25 ± 0.26	3.27 ± 0.43	3.24 ± 0.26	3.68 ± 0.52 *	0.0012[b]
LVEDDi (mm/g)	0.30 ± 0.06	0.33 ± 0.03	0.28 ± 0.05	0.31 ± 0.04	0.39 ± 0.05 * #† ‡	< 0.0001[a]
LVESD (mm)	1.62 ± 0.31	1.74 ± 0.32	1.70 ± 0.44	1.68 ± 0.31	3.20 ± 0.68 * #† ‡	< 0.0001[b]
LVESDi (mm/g)	0.17 ± 0.04	0.18 ± 0.04	0.14 ± 0.03	0.16 ± 0.03	0.34 ± 0.07 * # †‡	< 0.0001[a]
FS (%)	43.5 ± 7.4	46.6 ± 7.7	48.7 ± 7.1	48.6 ± 6.3	14.0 ± 9.3 * # †‡	< 0.0001[b]
LVM (mg)	36.3 ± 9.1	35.2 ± 5.7	38.9 ± 11.9	41.6 ± 12.0	49.8 ± 13.5	0.029[b]
LVMi (mg/g)	3.7 ± 0.7	3.6 ± 0.4	3.3 ± 0.8	3.9 ± 0.9	5.2 ± 1.1 * # †‡	< 0.0001[a]

χ Chi^2 test was used to assess the M/F distribution (χ); ANOVA, ordinary One-Way followed with Bonferroni Test for pairwise comparison ([a]), or Kruskal-Wallis with Dunn's Test correction for multiple comparison([b]) were used, where:

WT *vs Myh6*-Cre:*Lmna*$^{F/F}$: * $p < 0.05$

Myh6-Cre:*Lmna*$^{W/F}$ *vs Myh6*-Cre:*Lmna*$^{F/F}$: # $p < 0.05$

Lmna$^{F/F}$ *vs Myh6*-Cre:*Lmna*$^{F/F}$: † $p < 0.05$

Myh6-Cre *vs Myh6*-Cre:*Lmna*$^{F/F}$: ‡ $p < 0.05$

Abbreviations: HR, heart rate; bpm, beats per minute; ST, interventricular septal thickness; PWT, posterior wall thickness; LVEDD, left ventricular end diastolic diameter; LVEDDi, LVEDD indexed to body weight;

LVESD, left ventricular end systolic diameter; LVESDi, LVESD indexed to body weight; FS, fractional shortening; LVM, left ventricular mass; LVMi, LVM indexed to body weight.

Online Table 2

Echocardiographic parameters in WT, *Myh6-Cre* and *Myh6-Cre:Lmna*$^{W/F}$ mice at 10 months of age.

	WT	*Myh6*-Cre	*Myh6*-Cre:*Lmna*$^{W/F}$	p
N	22	12	18	N/A
M/F	12/6	7/5	13/5	0.73$^{\chi}$
Age (Months)	9.3 ± 0.7	8.8 ± 1.5	9.6 ± 0.6	0.77[b]
BW (g)	35.1 ± 6.3	35.0 ± 5.5	43.1 ± 8.5*#	0.002[a]
HR (bpm)	503 ± 80	489 ± 74	478 ± 70	0.57[a]
ST (mm)	0.62 ± 0.08	0.61 ± 0.04	0.64 ± 0.10	0.19[a]
PWT (mm)	0.66 ± 0.06	0.62 ± 0.03	0.65 ± 0.15	0.12[b]
LVEDD	3.9 1 ± 0.57	4.28 ± 0.35	4.92 ± 0.70*#	<0.0001[a]
LVEDDi (mm/g)	0.11 ± 0.02	0.12 ± 0.02	0.12 ± 0.02	0.32[a]
LVESD (mm)	1.9 ± 0.63	2.64 ± 0.35*	3.95 ± 1.01 *#	<0.0001[a]
LVESDi (mm/g)	0.06 ± 0.02	0.08 ± 0.02*	0.09 ± 0.02*	<0.0001[b]
FS (%)	51.6 ± 10.4	38.4 ± 5.7*	20.9 ± 10.8*#	<0.0001 [b]
LVM (mg)	70.5 ± 17.8	77.1 ± 12.9	104.5 ± 23.7*#	<0.0001[a]
LVMi (mg/g)	1.96 ± 0.38	2.22 ± 0.38	2.49 ± 0.58*	0.003 [a]

χ Chi^2 test was used to assess the M/F distribution; ANOVA, ordinary One-Way followed with Bonferroni Test for pairwise comparison ([a]), or Kruskal-Wallis with Dunn's Test correction for multiple comparison ([b]) were used, where:
WT *vs Myh6*-Cre:*Lmna*$^{W/F}$: * $p < 0.05$
Myh6-Cre:*Lmna*$^{W/F}$ *vs Myh6*-Cre: # $p < 0.05$
Myh6-Cre *vs* WT: ‡ $p < 0.05$

Abbreviations: as in Online Table 1.

Online Table 3

Cardiac arrhythmias in WT, *Lmna*$^{F/F}$, *Myh6-Cre, Myh6-Cre:Lmna*$^{W/F}$, and *Myh6-Cre:Lmna*$^{F/F}$ at 3 weeks of age

		WT	*Lmna*$^{F/F}$	*Myh6*-Cre	*Myh6*-Cre:*Lmna*$^{W/F}$	*Myh6*-Cre:*Lmna*$^{F/F}$	*p* value
N		14	10	10	19	19	
M/F		8/6	5/5	4/6	12/7	9/10	0.89[χ]
Age (days)		20.7 ± 1.2	21.4 ± 0.5	20.8 ± 0.7	20.8 ± 1.0	20.5 ± 0.9	0.078[(b)]
BW (g)		9.0 ± 1.3	11.5 ± 2.0*	10.7 ± 2.0*	10.5 ± 1.6*	8.8 ± 1.0†‡#	<0.0001[(a)]
Average recorded time (min)		42.5 ± 23.5	47.2 ± 19.2	27.0 ± 7.0	40.5 ± 20.9	32.5 ± 13.9	0.13[(b)]
Normal Sinus Rhythm		14 (100%)	10 (100%)	10 (100%)	19 (100%)	5 (15.8%)*#†‡	<0.0001[(b)]
Supra-ventricular arrhythmias	PAC	9 (64.3%)	8 (80%)	6 (60%)	14 (73.7%)	9 (47.4%)	0.72[(b)]
	AFib/ Flutters	0	0	0	0	6 (31.6%)*#†‡	0.0012[(b)]
	Other SVTs	0	0	0	0	9 (47.4%)*#†‡	<0.0001[(b)]
Atrio-ventricular block	1st degree AVB	0	0	0	0	3 (15.8%)	0.076[(b)]
	2nd degree AVB	0	1 (10%)	0	1 (5.3%)	11 (57.9%)*#†‡	<0.0001[(b)]
	3rd degree AVB/ Complete Heart Block	0	0	0	0	11 (57.9%)*#†‡	<0.0001[(b)]
Ventricular arrhythmias	PVC	0	2 (20%)	2 (20%)	5 (26.3%)	14 (73.7%)*	0.0005[χ]
	PVC (per mouse/h)	0	0.3	0.4	1.2	35.2	<0.0001[χ]
	VT	0	0	0	0	6 (31.6%) *#	0.0052

χ Chi^2 test was used to assess the M/F distribution; ANOVA, ordinary One-Way followed with Bonferroni Test for pairwise comparison ([a]), or Kruskal-Wallis with Dunn's Test correction for multiple comparison ([b]) were used, where:

WT *vs Lmna*$^{F/F}$*, Myh6*-Cre, *Myh6*-Cre:*Lmna*$^{W/F}$ and *Myh6*-Cre:*Lmna*$^{F/F}$: * $p < 0.05$
Myh6-Cre:*Lmna*$^{W/F}$ *vs Myh6*-Cre:*Lmna*$^{F/F}$: # $p < 0.05$
Lmna$^{F/F}$*vs Myh6*-Cre:*Lmna*$^{F/F}$: † $p < 0.05$
Myh6-Cre *vs Myh6*-Cre:*Lmna*$^{F/F}$: ‡ $p < 0.05$

Abbreviations: M/F: Male/Female; BW: Body weight; min: minute; PAC, Premature atrial contraction; AFib/Flutters, Atrial Fibrillation/atrial flutters; SVT, Supra-ventricular tachycardia; AVB, Atrioventricular block; PVC, Premature ventricular contraction; VT, Ventricular tachycardia (≥ 3 PVCs in the row).

.

Online Table 4

Cardiac Arrhythmias in WT, *Myh6-Cre* and *Myh6-Cre:Lmna*$^{W/F}$ at 8 to 10 months of age.

		WT	*Myh6*-Cre	*Myh6*-Cre:*Lmna*$^{W/F}$	*p* value
N		16	12	19	
M/F		9/7	7/5	13/6	0.73$^{\chi}$
Age (month)		10.1 ± 1.9	8.8 ± 1.6	9.4 ± 1.1	0.81$^{(b)}$
BW (g)		32.9 ± 3.4	35.0 ± 5.3	42.6 ± 8.4*#	<0.0001$^{(a)}$
Average recorded time (min)		24.5 ± 12.9	36.7 ± 8.4 *	38.1 ± 23.7	0.034$^{(b)}$
Normal Sinus Rhythm		11 (68.8%)	7 (58.3%)	7 (36.8%) *	0.011$^{(b)}$
Supra-ventricular Arrhythmias	**Sinus Pause**	0	0	2 (10.5%)	0.51$^{(b)}$
	PAC	13 (81.3%)	10 (83.3%)	16 (84.2%)	0.98$^{(b)}$
	A. Fib./Flutter	0	0	1 (5.26)	0.48$^{(b)}$
	SVT	2 (12.5%)	3 (25%)	6 (31.6%)	0.42$^{(b)}$
Atrio-Ventricular block	**2nd degree AV-B**	0	1 (8.3%)	7 (36.8%) *	0.01$^{(b)}$
	3rd degree AV-B	0	0	0	
Ventricular Arrhythmias	**PVC**	2 (12.5%)	8 (66.7%) *	16 (41.7%) *	0.0002$^{(b)}$
	PVC (per mouse/h)	0.6	1.5	41.7	<0.0001$^{\chi}$
	VT	0	0	2 (12.5%)	0.48$^{(b)}$

χ Chi^2 test was used to assess the M/F distribution; ANOVA, ordinary One-Way followed with Bonferroni Test for pairwise comparison (^{a}), or Kruskal-Wallis with Dunn's Test correction for multiple comparison (^{b}) were used, where:

WT *vs* *Myh6*-Cre and *Myh6*-Cre:*Lmna*$^{F/F}$: * $p < 0.05$

Myh6-Cre *vs* *Myh6*-Cre:*Lmna*$^{F/F}$: # $p < 0.05$

Abbreviations as in Online Table 3.

Online Table 5

Echocardiographic parameters in WT and *Myh6-Cre:Lmna*$^{F/F}$ mice at 2 weeks of age.

	WT	***Myh6*-Cre:*Lmna*$^{F/F}$**	*p* value
N	10	8	N/A
M/F	4/6	5/3	0.64$^{\chi}$
Age (days)	14 ± 0.9	15 ± 0.8	0.22[b]
BW (g)	7.7 ± 1.4	7.5 ± 1.1	0.75[a]
HR (bpm)	505 ± 65	544 ± 76	0.27[a]
ST (mm)	0.56 ± 0.10	0.51 ± 0.05	0.24[a]
PWT (mm)	0.57 ± 0.11	0.51 ± 0.05	0.20[a]
LVEDD	2.52 ± 0.16	2.67 ± 0.35	0.24[a]
LVEDDi (mm/g)	0.34 ± 0.05	0.36 ± 0.03	0.38[b]
LVESD (mm)	1.27 ± 0.22	1.39 ± 0.30	0.33[a]
LVESDi (mm/g)	0.17 ± 0.04	0.19 ± 0.03	0.30[a]
FS (%)	49.8 ± 6.0	48.2 ± 5.4	0.56[a]
LVM (mg)	28.1 ± 8.1	27.2 ± 7.3	0.93[a]
LVMi (mg/g)	3.7 ± 1.0	3.6 ± 0.7	0.80[a]

χ Chi^2 test was used to assess the M/F distribution; Unpaired t test ([a]), or Mann-Whitney test ([b]) were used, where:
WT *vs Myh6*-Cre:*Lmna*$^{F/F}$: * $p < 0.05$
Myh6-Cre *vs Myh6*-Cre:*Lmna*$^{F/F}$: ‡ $p < 0.05$

Abbreviations as in Online Table 1.

Online Table 6
Predicted dysregulated upstream transcriptional regulators

Upstream Regulators (Growth factors)	*p* value (overlap of DEGs with genes in the pathway)	Upstream Regulators (Transcription factors)	*p* value (overlap of DEGs with genes in the pathway)
TGFB1	0.000000625	TP73	0.000000784
ANGPT1	0.0000774	SP1	0.00000128
GDF15	0.0000892	KLF15	0.0000167
VEGFA	0.000408	ATF7	0.0000211
FGF1	0.000923	TP53	0.0000381
KITLG	0.00138	EGR1	0.0000506
AGT	0.0028	PAX3	0.0000861
FGF19	0.0043	SMARCA4	0.000152
ANGPT2	0.00568	IRX4	0.000259
BMP10	0.00607	STAT6	0.000275
INHA	0.0132	SRF	0.000306
LEP	0.0161	RCAN1	0.000336
HGF	0.0184	SP3	0.000754
VEGFB	0.0192	HMGB1	0.000985
TDGF1	0.0227	MYOD1	0.00105
GDF10	0.024	TCL1A	0.00133
IGF1	0.0256	CREBBP	0.00143
FGF21	0.0258	EPAS1	0.00144
CCN2	0.0423	STAT3	0.00147
		STAT5B	0.00157
		ZNF219	0.00169
		NFKBIA	0.00245
		TCF7L2	0.00271
		STAT1	0.00338
		FOXA2	0.00382
		KDM5A	0.00414
		Esrra	0.00423
		NFE2L2	0.00464
		SP2	0.00502
		RB1	0.00655
		IRF8	0.007
		GATA6	0.00731
		HEY2	0.00769
		IRF6	0.00798
		Msx3	0.00806
		NFKBIB	0.00934
		EP300	0.00983
		HMGA1	0.00989
		TBX5	0.0117
		TFAP2A	0.012
		HDAC5	0.0124
		MRTFA	0.0126
		MTPN	0.0139

		MEF2C	0.0149
		KLF3	0.015
		SOX4	0.015
		PDX1	0.0161
		HIF1A	0.0167
		JUNB	0.0169
		MRTFB	0.0176
		CDKN2B	0.0185
		ETS1	0.0186
		SATB1	0.0196
		MYOCD	0.0211
		EBF2	0.0213
		ID3	0.0221
		SMAD1	0.0224
		CALR	0.0224
		NFKBIE	0.0227
		HTT	0.0238
		CAMTA2	0.024
		ZNF260	0.024
		EGR3	0.0241
		MEF2A	0.0241
		Foxp1	0.0241
		ATF2	0.0255
		MYC	0.0256
		TFE3	0.0258
		ECSIT	0.0261
		TEAD1	0.0263
		Ncoa6	0.0273
		TEAD3	0.0277
		ARNT2	0.0281
		HOXA9	0.0281
		KLF4	0.0295
		HOXA3	0.0296
		FOS	0.0308
		SMAD4	0.0314
		SP4	0.0315
		KLF2	0.0317
		CIC	0.0323
		ETV6	0.0323
		GATA5	0.0323
		HOXA10	0.0327
		SIM1	0.0332
		NFKB1	0.0349
		RELA	0.0367
		IRF4	0.0369
		BCL6	0.037
		MYOG	0.0374

		SMAD5	0.0374
		LHX1	0.0391
		SREBF1	0.0423
		WWTR1	0.0426
		EBF1	0.0427
		PIAS4	0.0431
		CBL	0.045
		CEBPA	0.0461
		HLTF	0.0474
		CCNT2	0.0474
		ING2	0.0474
		TBX3	0.049

Abbreviation: DEGs: Differentially expressed genes

Online Table 7

Cardiac Arrhythmias in WT and untreated, vehicle-treated and JQ1-treated *Myh6-Cre:Lmna*$^{F/F}$ mice at 3 weeks of age

		WT	*Myh6*-Cre:*Lmna*$^{F/F}$	*Myh6*-Cre:*Lmna*$^{F/F}$	*p* value
Treatment		**Untreated**	**Untreated & Vehicle treated**	**JQ1**	
N		14	23	14	
M/F		8/6	11/12	7/7	0.93[χ]
Age (days)		20.7 ± 1.2	20.5 ± 0.8	20.5 ± 0.5	0.55[b]
BW (g)		8.9 ± 1.3	8.9 ± 1.0	8.3 ± 0.8	0.14[a]
Average recorded time (min)		42.5 ± 23.5	31.7 ± 12.8	33.5 ± 16.5	0.19[a]
Normal Sinus Rhythm		14 (100%)	5 (21.7%) *	7 (50%) *	<0.0001[b]
Supra-ventricular Arrhythmias	**PAC**	9 (64.3%)	9 (39.1%)	2 (18.2 %) *	0.074[b]
	A.Fib./ Flutters	0	8 (34.8%) *	0 †	0.0035[b]
	SVT	0	12 (52.2%) *	1 (9.1%) †	<0.0001[b]
Atrio-Ventricular block	**2nd degree AVB**	0	14 (65.2%) *	5 (45.5%)	0.001[b]
	3rd degree AVB/ Complete Heart Block	0	15 (69.6%) *	5 (45.5%)	0.0005[b]
Ventricular Arrhythmias	**PVC**	0	17 (73.9%) *	8 (72.7%) *	<0.0001[b]
	PVC (Per mouse/h)	0	32	16	<0.0001[χ]
	VTs	0	6 (31.6%)	0	0.017[b]

χ Chi^2 test was used to assess the M/F distribution; ANOVA, ordinary One-Way followed with Bonferroni Test for pairwise comparison ([a]), or Kruskal-Wallis with Dunn's Test correction for multiple comparison ([b]) were used, where:

Untreated WT *vs* *Myh6*-Cre:*Lmna*$^{F/F}$ or JQ1-treated *Myh6*-Cre:*Lmna*$^{F/F}$: * $p < 0.05$
Myh6-Cre:*Lmna*$^{F/F}$ *vs* JQ1-treated *Myh6*-Cre:*Lmna*$^{F/F}$: † $p < 0.05$

Abbreviations as per Online Table 3.

Online Table 8

A. Genotyping primers list:

Gene	Forward sequence	Reverse sequence
Lmna Flox	TCGAGGCTCTTCTCAACTCC	CTCTCCTCTGAAGTGCTTGGA
Cre recombinase	GCGGTCTGGCAGTAAAAACTATG	GTGAAACAGCATTGCTGTCACTT
Internal control	CTAGGCCACAGAATTGAAAGATCT	GTAGGTGGAAATTCTAGCATCATCC

B. qPCR primers list:

SYBR Green primer list:

Gene	Forward sequence	Reverse sequence
Slc24a2	GCTAATTCGAGTCATTGGCCT	TGTTGCTCTGAGAGTCTGTCT
Plvap	GCTGGTACTACCTGCGCTATT	CCTGTGAGGCAGATAGTCCA
Col6a2	AAGGCCCCATTGGATTCCC	CTCCCTTCCGACCATCCGAT
Clmp	GAACTAAGCCCATTGTGTAT	AGGGTTGTTGTAATCAATTC
Cercam	GACTATGCGACTGTCGTCTGG	ACTGATGCCGTTCTTTGGTCC
Fzd2	GCCGTCCTATCTCAGCTATAAGT	TCTCCTCTTGCGAGAAGAACATA
Slc7a2	TCTATGTTCCCCTTACCCCGA	TGACTGCCTCTTACTCACTCTT
Syt17	GTCAGAGGTGCTATGAGTCCA	GGGGTCAAAGGAACATCGCT
Fam114a1	TGATGCTCGTGACACCATAGC	CTGGACCACACTGCACTTCT
Adamts19	CCAGATGCCTCCTGCTTTTAC	GGTGCGGGTGACCTATGAT
Fads1	AGCACATGCCATACAACCATC	TTTCCGCTGAACCACAAAATAGA
Ikbke	ACCACTAACTACCTGTGGCAT	CCTCCCCGGATTTCTTGTTTC
Fgl2	GGTGCTCAAAGAAGTGCGGA	GTTCCTGGACTCTACTGTCCTC
Adamtsl3	CCAGAAGTCTCTAATCCAGTGGG	AATGAGCTTGAGAACGACCGT
Col1a1	GCTCCTCTTAGGGGCCACT	CCACGTCTCACCATTGGGG
Col1a2	TTCTGTGGGTCCTGCTGGGAAA	TTGTCACCTCGGATGCCTTGAG
Col3a1	CTGTAACATGGAAACTGGGGAAA	CCATAGCTGAACTGAAAACCACC
Col4a3	GTATGTAACTTTGCATCACG	ATCTGCTAATATAGGGTTCG
Col5a1	CTTCGCCGCTACTCCTGTTC	CCCTGAGGGCAAATTGTGAAAA
Col5a2	TTGGAAACCTTCTCCATGTCAGA	TCCCCAGTGGGTGTTATAGGA
Col6a2	AAGGCCCCATTGGATTCCC	CTCCCTTCCGACCATCCGAT
Col14a1	TTTGGCGGCTGCTTGTTTC	CGCTTTTGTTGCAGTGTTCTG
Tgfb2	GAGCTCGTGGTCTTAGTAAC	CGGAGCAGAGTTTTATATGT
Ctgf	GTGCTCCTCGCTCTCT	GAGGTCAGTCTGTGATCG
Col12a1	AAGTTGACCCACCTTCCGAC	GGTCCACTGTTATTCTGTAACCC
Tgfb1	ACTGGAGTTGTACGGCAGTG	GGGGCTGATCCCGTTGATTT
Col6a3	GCTGCGGAATCACTTTGTGC	CACCTTGACACCTTTCTGGGT
Vcan	ACTAACCCATGCACTACATCAAG	ACTTTTCCAGACAGAGAGCCTT
Sox9	AGTACCCGCATCTGCACAAC	ACGAAGGGTCTCTTCTCGCT
Rcn3	ATGATGTGGCGATGGTCGTTT	CGTACTGGAAATTCCCGTGGG
Myof	ACCGCTTTCGGTGTGATCC	GCCAGTAATGGTTTGGTGTCTTC
Plcq3	ATGGGAACGTGAAGCAAGC	AATTGTCAAGTCATTGGTGGTCA
Cgref1	ATGCTGCCACTATTGCTGCT	TCCATCTTCTCTAGTCCCTTGAG
Ahnak2	CCTGTGCAGGCCTGTGTGTATAC	GTATCCATGCCAGAGACCTTAAC
Fhl1	GACTGCCGCAAGCCCATAA	CCAAGGGGTGAAGGCACTT

Phlda3	CCGTGGAGTGCGTAGAGAG	TCTGGATGGCCTGTTGATTCT
Rasl11b	TGTGTACCATCGCAGAGTACC	TGAGGAATCGGACCACCAAAG
Pamr1	ACGTGAAGGGATTCTACTGCG	CGTTTAAGGGATAGCTCTCCAAC
Plag2g4a	CAGCACATTATAGTGGAACACCA	AGTGTCCAGCATATCGCCAAA
Ssc5d	AGGCTTCACTGTCAGAATGCCC	GCTCCAACTGAAAGGGTCTGAG
Bcl2	ATGCCTTTGTGGAACTATATGGC	GGTATGCACCCAGAGTGATGC
Bcl2l11	CCCGGAGATACGGATTGCAC	GCCTCGCGGTAATCATTTGC
Bbc3	ACGACCTCAACGCGCAGTACG	GTAAGGGGAGGAGTCCCATGAAG
Gadd45a	CCGAAAGCATGGACACGGTG	TTATCGGGGTCTACGTTGAGC
Gadd45b	CAACGCGGTTCAGAAGATGC	GGTCCACATTCATCAGTTTGGC
Gadd45g	GGGAAAGCACTGCACGAACT	AGCACGCAAAAGGTCACATTG
Tnfsf10	ATGGTGATTTGCATAGTGCTCC	GCAAGCAGGGTCTGTTCAAGA
Stk38L	ACTTGGCCTAGATGACTTTGAGT	GATGTGCCCCGTGTCTTTCTT
Gapdh	AAGATGGTGATGGGCTTCCCG	TGGCAAAGTGGAGATTGTTGC
ChIP primers to be added		

Taqman probes:

Gene	Probe reference
Nppa	Mm1255747-g1
Nppb	Mm01255770-g1
Myh6	Mm00440354-m1
Myh7	Mm00600555-m1
Atp2a2	Mm00437634-m1
Actc1	Mm01333821-m1
Gapdh	Mm99999915-g1

C. List of Antibodies

Protein	Manufacturer	Catalogue #	Usage
LMNA	Abcam	ab26300	WB
LMNA	Santa-Cruz	E-1 sc-376248	IF
PCM1	Sigma	HPA023370	IF
BRD4	Bethyl	A301-985A100	ChIP, WB
BRD3	Bethyl	A302-368A	WB
BDR2	Bethyl	A302-583A	WB
TGFβ1	R&D System	MAB1835	WB
CTGF	Santa-Cruz	E-5 sc-365970	WB
αTUBULIN	Cell Signaling Technology	11H10 #2125	WB
GAPDH	Abcam	ab8245	WB
Rabbit IgG	BD	3109265	ChIP

Anti-mouse IgG HRP	Cell Signaling Technology	# 7076	WB
Anti-rabbit IgG HRP	Cell Signaling Technology	# 7074	WB
Donkey anti-Mouse IgG, Alexa Fluor 488	Invitrogen	A21202	IF
Donkey anti-Rabbit IgG, Alexa Fluor 594	Invitrogen	A21207	IF